15 CREEP AND VISCOPLASTICITY

In the following chapter, we will discuss the *classical creep* theories for steel and metals, as well as the general formulations for creep and *viscoplasticity*. In these formulations - and in contrast with viscoelasticity - it is characteristic that the time-dependent strains are nonproportionally related to the stresses.

The classical creep theories for steel and metals are of relevance when the loading is below the initial yield stress. In that case, it turns out that in addition to the elastic strain, a sufficiently high temperature - and stress - will also give rise to a creep strain, i.e.

$$\boxed{\varepsilon = \varepsilon^e + \varepsilon^{cr}} \tag{15.1}$$

The question then arises what a 'sufficiently' high temperature means, and, according to Ashby and Jones (1980), it is found for metals and steel that

$$\boxed{\frac{\theta}{\theta_M} > 0.3 - 0.4 \quad \Rightarrow \quad creep}$$

where θ is the absolute temperature $[K]$ and θ_M is the melting temperature; for ceramics it is found that a temperature of $\theta/\theta_M > 0.4 - 0.5$ is required for development of creep strains. The ratio θ/θ_M is called the *homologous temperature*. For lead $\theta_M \approx 600\,K$ and at room temperature we therefore have $\theta/\theta_M \approx 0.5$ and lead pipes in old buildings are therefore often found to exhibit significant creep deformations. For steel, $\theta_M \approx 1800\,K$ and creep is therefore of importance when the temperature is above $270 - 450\,^oC$.

General reviews of classical creep theories for steel and metals, are given by Finnie and Heller (1959), Lubahn and Felgar (1961), Odqvist and Hult (1962), Nadai (1963), Odqvist (1966), Hult (1966), Rabotnov (1969) and Stouffer and Dame (1996).

15.1 Results based on the standard creep test

For a standard creep test performed at the constant temperature θ and where the constant tensile stress σ is applied instantaneously, we have $\varepsilon^{cr} = \varepsilon^{cr}(\sigma, \text{load}$

history, θ) and as the load history is uniquely related to the loading time t, we can write

$$\varepsilon^{cr} = \varepsilon^{cr}(\sigma, t, \theta)$$

Frequently, however, it is assumed that the influence of stress, loading time and temperature can be factorized, i.e.

$$\varepsilon^{cr} = f(\sigma)g(t)h(\theta) \tag{15.2}$$

It is characteristic for creep of steel and metals that ε^{cr} for stress states of engineering importance depends nonlinearly on stress and most often a *power law* is adopted, i.e.

$$f(\sigma) \sim (\frac{\sigma}{\sigma^*})^n \tag{15.3}$$

as proposed by Norton (1929) and Bailey (1929). Here the *creep exponent* $n \geq 1$ is usually in the range of 3-8, cf. Ashby and Jones (1980), and σ^* is an arbitrary, positive reference stress that we choose with the sole purpose of making the expression dimensionless; in the literature, this power law is often called *Norton's law*. A number of other expressions is available, for instance $f(\sigma) \sim e^{B\sigma} - 1$, where the parameter B is positive, as proposed by Soderberg (1936), and $f(\sigma) \sim sinh(C\sigma)$, where the parameter C is positive, as proposed by Prandtl (1928) and Nadai (1938). For larger stresses, these two expressions coincide in the limit; moreover, for small stresses both expressions provide a linear stress dependence and we will return to this aspect later. In practice, both the power law, the exponential law and the hyperbolic sine law can - within a certain stress range - closely approximate experimental data, but the power law is the expression commonly used. For a more detailed discussion and comparison of these expressions, the reader may consult Nadai (1963), Odqvist (1966) and Rabotnov (1969).

The influence of loading time is often modeled through the simple expression

$$g(t) \sim (\frac{t}{t^*})^m \tag{15.4}$$

where $0 < m \leq 1$; it appears that $0 < m < 1$ corresponds to primary creep and $m = 1$ to secondary creep. Moreover, t^* is an arbitrary reference time we choose with the sole purpose that the expression becomes dimensionless. Expression (15.4) has the drawback that either primary creep ($0 < m < 1$) or secondary creep $m = 1$ is considered. A format which allows primary and secondary creep to be considered in one and the same expression was proposed by McVetty (1934) and it reads $\varepsilon^{cr} = f(\sigma, \theta)(1 - e^{-at}) + g(\sigma, \theta)t$, where a is a positive parameter. It appears that when $t \to \infty$ then $\dot{\varepsilon}^{cr} \to g(\sigma, \theta)$ where $g(\sigma, \theta)$ is the secondary creep rate.

Finally, the influence of temperature is most often modeled via the *law of Arrhenius*, i.e.

$$h(\theta) \sim e^{-\frac{Q}{R\theta}} \tag{15.5}$$

where R is the *universal gas constant* = 8.314 $[\frac{\text{J}}{\text{mol}\,K}]$ and Q is the *activation energy* for creep [J/mol]. The reason for this choice is that, as we will discuss later, creep development is closely related to diffusion processes and the temperature influence on diffusion processes is controlled by the law of Arrhenius, cf. for instance Ashby and Jones (1980).

Certainly, there exist other relations for $f(\sigma)$, $g(t)$ and $h(\theta)$ than those discussed above - reviews are given by Altenbach (1999), Boresi and Sidebottom (1972) and Stouffer and Dame (1996) - but the expressions we have chosen are the ones most often adopted. Combining (15.2) with (15.3)-(15.5) we obtain

$$\varepsilon^{cr} = A(\frac{\sigma}{\sigma^*})^n(\frac{t}{t^*})^m e^{-\frac{Q}{R\theta}} \tag{15.6}$$

where A is a positive dimensionless material parameter. It is recalled that σ^* and t^* are an arbitrary positive reference stress and reference time respectively, that we choose with the sole purpose of obtaining a convenient dimension of the parameter A. Once σ^* and t^* have been chosen, (15.6) involves the four material parameters A, n, m and Q. Expression (15.6) holds for a creep test where σ is a tensile stress and in order that a compressive creep test is also allowed for, (15.6) is rewritten as

$$\boxed{\begin{array}{l}\varepsilon^{cr} = A(\frac{|\sigma|}{\sigma^*})^{n-1}\frac{\sigma}{\sigma^*}(\frac{t}{t^*})^m e^{-\frac{Q}{R\theta}} \\ \textit{where } \sigma^* \textit{ and } t^* \textit{ are arbitrary positive reference quantities}\end{array}} \tag{15.7}$$

In practice, secondary creep is often of great practical interest. If the stress and temperature are kept constant over a long period, secondary creep will occur and this is the dominant creep mechanism in, for instance, a steam generator at a power station which in practice operates under stationary conditions over very long periods. Much research has therefore focused on secondary creep and how temperature and stress, for a given material, influence the creep behavior. Research within material science has identified some characteristic creep mechanisms in steel and metals that will be discussed shortly; for a more detailed discussion the reader may consult Gittus (1975), Ashby and Jones (1980), Evans and Wilshire (1993) and Stouffer and Dame (1996).

For secondary creep, it turns out that creep for small stresses may occur due to so-called *diffusional creep* where atoms and vacancies are transported by means of diffusion; in *Nabarro-Herring creep* this transport occurs through the grains whereas in *Coble creep* it occurs along the grain boundaries. It turns out

that diffusional creep depends almost linearly on stress, i.e. the creep exponent in (15.6) is $n \approx 1$.

Still considering secondary creep, but now evaluating creep development for large stresses, another type of creep process becomes dominant - this is the so-called *dislocation creep* mechanism. From the field of material science, it is recalled that plastic strains in steel and metals develop due to movements of *dislocations*; a dislocation being an irregularity in the arrangement of atoms in the crystal lattice. When a dislocation meets an obstacle (dissolved solute atoms, vacancies, etc.), an increased stress is necessary to move the dislocation further and this is what happens in hardening plasticity. However, when exposed to the same stress over a long time - as it occurs in the standard creep test - another possibility for the motion of the dislocation emerges; namely that due to diffusional processes, the dislocation becomes able to 'climb' over the obstacle. Therefore, dislocation creep is also referred to as *dislocation climb* whereas plasticity (in steel and metals) is due to *dislocation glide*. It is characteristic that dislocation creep results in a strongly nonlinear dependence of the stress, and theoretical considerations within material science suggest that the creep exponent in Norton's law is $n \approx 4$.

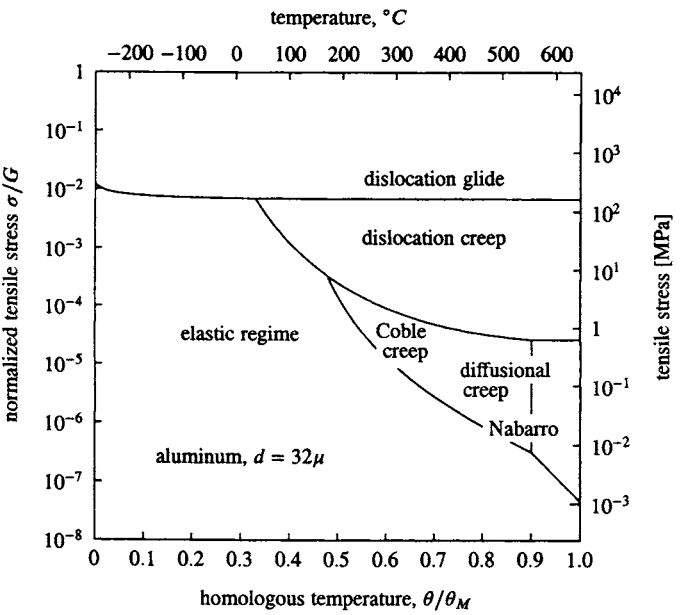

Figure 15.1: Deformation mechanism map for aluminum (grain diameter d = 32 μm), Gittus (1975); secondary creep is considered.

Information of how the stress and temperature influence the dominant de-

formation mechanisms for a particular material can be conveniently shown in a *deformation mechanism map*; as an example, Fig. 15.1 shows the result for aluminum. Above the curve 'dislocation glide', plasticity occurs and the dominant regions for elastic behavior, diffusional creep where $n \approx 1$ and dislocation creep where $n > 1$ appear from this figure; it is recalled that these creep regions refer to the occurrence of secondary creep data. Moreover, in Fig. 15.1 the boundary separating the elastic response from the creep regions is defined by $\dot{\varepsilon}^c = 10^{-8}[1/s]$. Deformation mechanism maps are available for a number of materials, see Gittus (1975) and Frost and Ashby (1982), and qualitatively they all have the same appearance as Fig. 15.1. Moreover, it turns out that the grain diameter d has a strong influence on the deformation mechanism map.

15.2 Uniaxial stress changes - Classical hardening rules

For a constant temperature, (15.6) can be written as

$$\varepsilon^{cr} = A(\frac{\sigma}{\sigma^*})^n(\frac{t}{t^*})^m \tag{15.8}$$

where the new parameter A has replaced the old term $Ae^{-\frac{Q}{RS}}$; moreover, for convenience only non-negative stresses are considered and the format (15.7) is then not needed. Expression (15.8) relates to the standard creep test where the stress is constant. Differentiation with respect to time gives

$$\dot{\varepsilon}^{cr} = \frac{mA}{t^*}(\frac{\sigma}{\sigma^*})^n(\frac{t}{t^*})^{m-1} \tag{15.9}$$

In plasticity theory it was argued that no unique relation exists between the stresses and strains, and the constitutive relations must therefore be of an incremental nature. In exactly the same fashion, we cannot expect that the creep strain for an arbitrary stress history only depends on the current stress value and loading time; if that were the case, the creep strain would then be independent of the load history. Therefore, when the stress changes during the load history, we must try to establish an expression for $\dot{\varepsilon}^{cr}$ and not for ε^{cr}.

Formally, (15.9) is identical to (15.8), but if (15.9) is now postulated to hold even when the stress is allowed to change during the load history, an expression for the creep strain rate has been achieved that holds for general uniaxial stress conditions. Since the creep strain rate changes - that is, hardens - as a function of time (unless $m = 1$ holds), (15.9) is a *time-hardening model*; this expression is easily generalized to the following format

$$\boxed{\dot{\varepsilon}^{cr} = f(\sigma, t) \quad \textit{time-hardening}} \tag{15.10}$$

where $f(\sigma, t)$ is some function. In relation to (14.17) and Fig. 14.25 we have already discussed time-hardening and argued that loading time in itself is a poor measure of hardening.

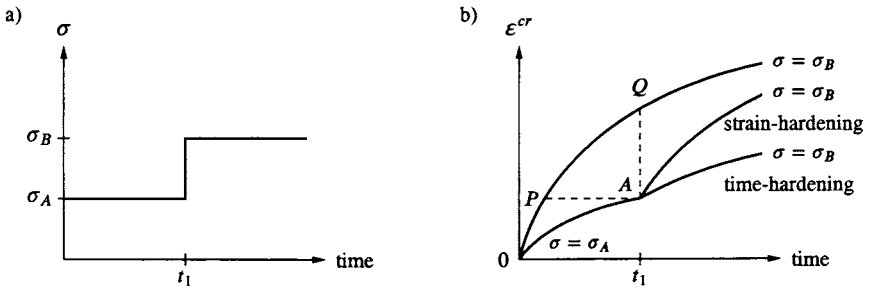

Figure 15.2: a) Stress history, b) creep strain predicted by time-hardening and strain-hardening.

However, another hardening possibility suggests itself. Eliminate the time t in (15.9) by means of (15.8) to obtain

$$\dot{\varepsilon}^{cr} = \frac{mA^{\frac{1}{m}}}{t^*}\left(\frac{\sigma}{\sigma^*}\right)^{\frac{n}{m}}(\varepsilon^{cr})^{\frac{m-1}{m}} \tag{15.11}$$

Again, this expression is identical to (15.8) for a constant stress, but now (15.11) is postulated to hold even when the stress changes during the loading history. Since the creep strain rate changes - i.e. hardens - as a function of the creep strain ε^{cr}, (15.11) is a *strain-hardening model*; it is easily generalized to

$$\boxed{\dot{\varepsilon}^{cr} = f(\sigma, \varepsilon^c) \quad \textit{strain-hardening}} \tag{15.12}$$

where $f(\sigma, \varepsilon^{cr})$ is a function. According to this model the creep strain ε^{cr} characterizes the state of the material and - in the spirit of Section 10.1 - it may therefore be viewed as an internal variable.

The strain-hardening model is certainly expected to be much more realistic than the time-hardening model, and the difference becomes significant when large stress changes occur. However, historically the time-hardening model has been used extensively due to its simplicity when deriving analytical solutions for structural elements.

To further substantiate the superiority of the strain-hardening model, consider the stress history in Fig. 15.2a). For a standard creep test with $\sigma = \sigma_B$, the creep strain curve OPQ in Fig. 15.2b) is obtained. For the actual stress history both models predict the same creep strain curve up to time $t = t_1$. At time $t = t_1$, the stress is suddenly increased to from $\sigma = \sigma_A$ to $\sigma = \sigma_B$ and according to the time-hardening model (15.10) the creep strain rate, i.e. the slope, at point A equals the creep strain rate at point Q. However, according to the strain-hardening model (15.12) the creep strain rate at point A equals that at point P. The expectation that the strain-hardening model is in closer agreement with experimental data than the time-hardening model is confirmed by numerous experiments for steel and metals, cf. Boresi and Sidebottom (1972) and Finnie and Heller (1959), and also for rock salt, see Ottosen and Krenk (1982).

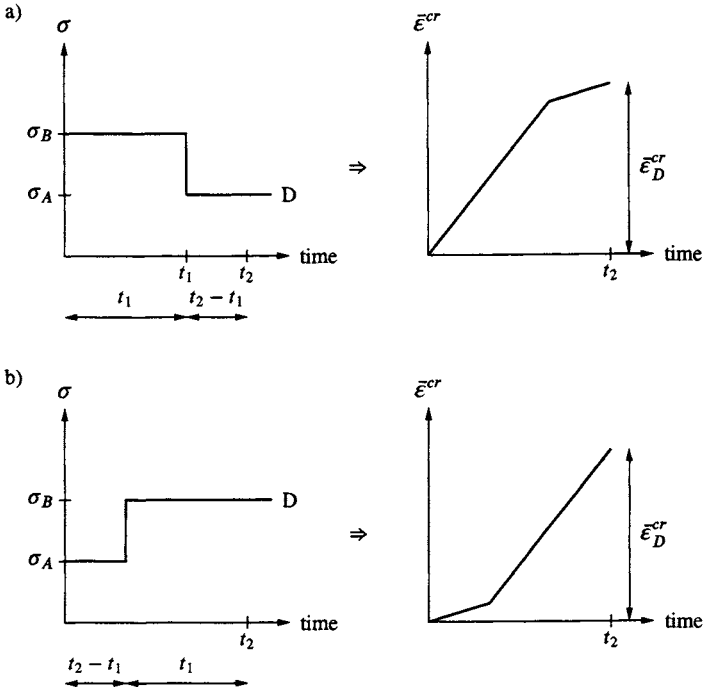

Figure 15.3: The factorized stain-hardening model exhibits no sequence effects; the load histories in a) and b) result in the same creep strain at point D (for simplicity, only secondary creep is involved).

In general, one may expect that the sequence with which the load is applied would influence the final creep strain; a small stress followed by a large stress is not expected to result in the same final creep strain as a large stress followed by a small stress, and this is confirmed by experiments, see Rabotnov (1969). The factorized strain-hardening model exhibits no such *sequence effects*. In the factorized form of the strain-hardening model, (15.12) takes the form

$$\boxed{\dot{\varepsilon}^{cr} = f(\sigma)g(\varepsilon^{cr}) \quad \textit{factorized strain-hardening model}} \tag{15.13}$$

where $f(\sigma)$ and $g(\varepsilon^{cr})$ are functions, cf. the similar structure in (15.11). Define now the variable $\bar{\varepsilon}^{cr}$ by

$$\dot{\bar{\varepsilon}}^{cr} = \frac{\dot{\varepsilon}^{cr}}{g(\varepsilon^{cr})}$$

and it is evident that the quantity $\bar{\varepsilon}^{cr}$ is related uniquely to the creep strain ε^{cr}. Then the factorized strain-hardening model (15.13) becomes

$$\dot{\bar{\varepsilon}}^{cr} = f(\sigma)$$

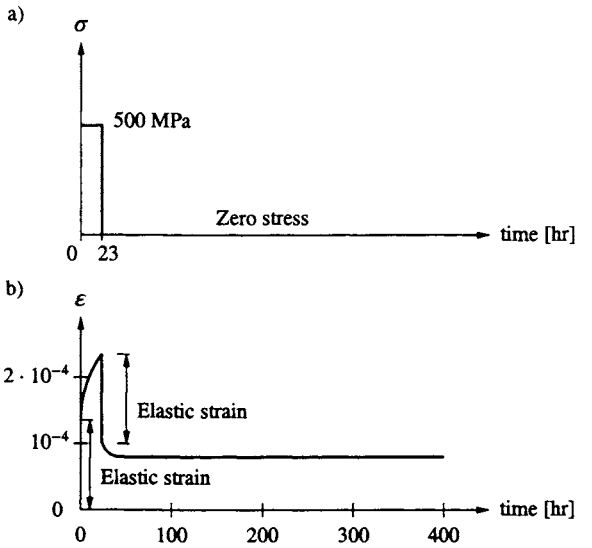

Figure 15.4: Creep and creep recovery of Cr-Mo-V steel at 425 °C, experimental results of Lubahn (1961).

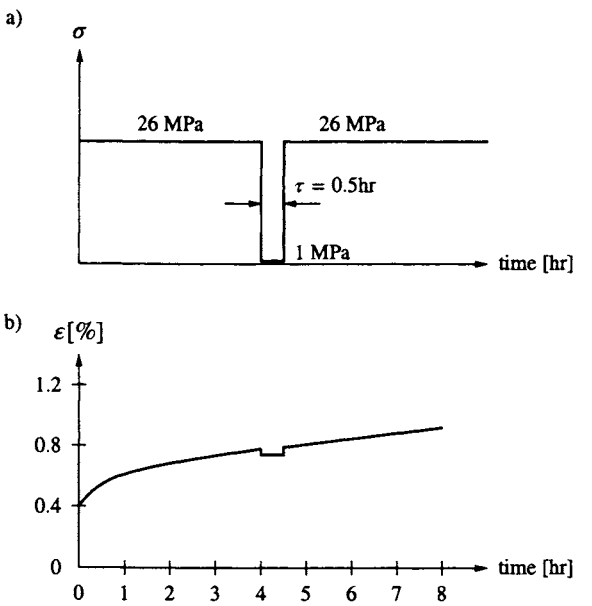

Figure 15.5: Interrupted creep test where the time of interruption is short (=0.5 hr); Al 1100 at 150 °C, experimental results of Wang and Onat (1968).

It appears that $\dot{\bar{\varepsilon}}^{cr}$ only depends on the current stress and not on the current value of $\bar{\varepsilon}^{cr}$ (and thereby not on the current value of ε^{cr}). It then follows that there can be no sequence effects. As an example, the factorized strain-hardening model will predict the same creep strain at point D in Fig. 15.3a) and b) where - for simplicity - only secondary creep is involved.

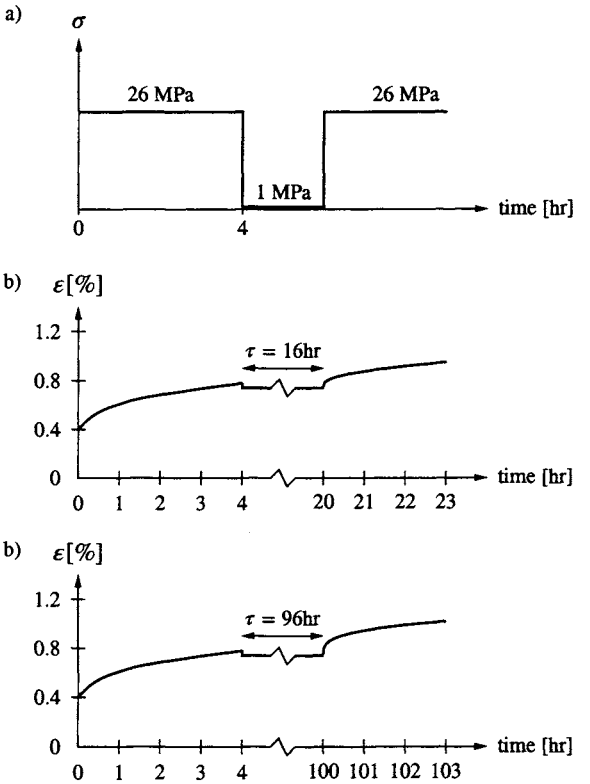

Figure 15.6: Interrupted creep test when the time of interruption is long; a) stress history, b) 16 hr interruption and c) 96 hr interruption; Al 1100 at 150 °C, experimental results of Wang and Onat (1968).

In linear viscoelasticity, creep recovery effects are often significant, see for instance Fig. 14.20. For steel and metals, however, this recovery effect is usually modest as shown in Fig. 15.4.

Recognizing the modest recovery, it would be tempting to expect that no significant changes occur during periods of total unloading. For the short unloading period (=0.5 hr) in Fig. 15.5 the material continues to creep after reloading as it did before. However, if the unloading period is longer the material exhibits significant primary creep upon reloading, cf. Fig. 15.6. It is therefore concluded that at intermediate or high temperature, the internal state of a metal or steel

changes even though it has been completely unloaded. Evidently, this change of the internal state cannot be predicted by the strain-hardening model.

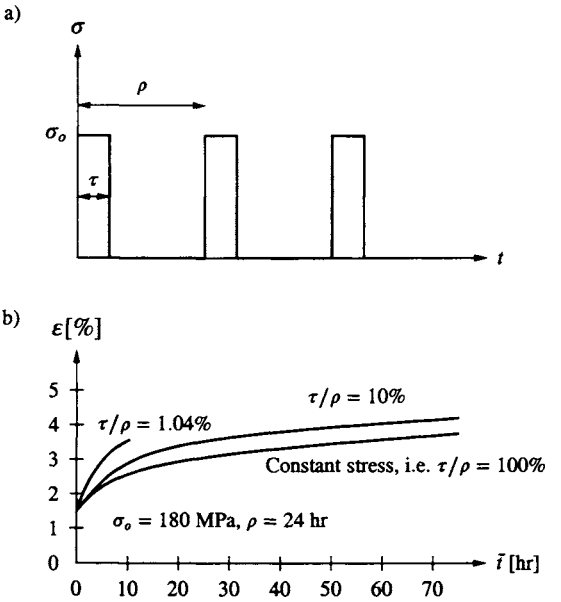

Figure 15.7: Creep of steel at 450 °C under periodically varying stress; a) stress history, b) experimental results reported by Onat and Fardshisheh (1972) where $\bar{t}$ is the reduced time, i.e. the total time spent under stress.

The effects discussed above become very evident when a periodically varying stress is applied. According to Fig. 15.7a), the period of the load is ρ and the duration of the load within each period is τ; the reduced time $\bar{t}$ measures the total time spent under stress. The corresponding experimental total strain ϵ is shown in Fig. 15.7b) and - intuitively somewhat surprisingly - it appears that the periodic loading gives rise to much larger strains than the constant load; again, this significant effect cannot be modeled by the strain-hardening model.

15.3 Multiaxial stress states

With this detailed discussion of the response for uniaxial stress conditions, it is timely to establish the multiaxial constitutive formulation. Let us as our point of departure take the strain-hardening model (15.11) written so that it applies not only to tensile stresses, but also to compressive stresses; we then have

$$\dot{\varepsilon}^{cr} = \frac{mA^{\frac{1}{m}}}{t^*}\left(\frac{|\sigma|}{\sigma^*}\right)^{\frac{n}{m}-1}\frac{\sigma}{\sigma^*}\left(|\varepsilon^{cr}|\right)^{\frac{m-1}{m}} \tag{15.14}$$

Moreover, (15.1) gives

$$\dot{\varepsilon} = \frac{\dot{\sigma}}{E} + \dot{\varepsilon}^{cr} \tag{15.15}$$

A comparison of (15.14) and (15.15) with (14.7) shows that the creep model takes the form of a nonlinear Maxwell model, i.e.

$$\dot{\varepsilon} = \frac{\dot{\sigma}}{E} + \frac{\sigma}{\eta(|\sigma|, |\varepsilon^{cr}|)} \tag{15.16}$$

where

$$\frac{1}{\eta(|\sigma|, |\varepsilon^{cr}|)} = \frac{mA^{\frac{1}{m}}}{t^*\sigma^*}\left(\frac{|\sigma|}{\sigma^*}\right)^{\frac{n}{m}-1}(|\varepsilon^{cr}|)^{\frac{m-1}{m}}$$

The next piece of information is that all experimental evidence shows that

For metals and steel the creep strains are incompressible, i.e. $\dot{\varepsilon}^{cr}_{ii} = 0$	(15.17)

and we note the complete similarity with the observations for plasticity.

For an isotropic material, the three-dimensional Maxwell model is given by (14.22) where it was concluded that the parameter ξ should be chosen as $\xi = \frac{1}{2}$ if (15.17) were to hold. We are then led to

$$\dot{\varepsilon}_{ij} = C_{ijkl}\dot{\sigma}_{kl} + \dot{\varepsilon}^{cr}_{ij} \quad \text{where} \quad \dot{\varepsilon}^{cr}_{ij} = \frac{3}{2\eta}s_{ij} \tag{15.18}$$

where C_{ijkl} is the elastic flexibility tensor. It is recalled that the viscosity parameter η depends on the stresses and the creep strains, i.e. $\eta = \eta(\sigma_{ij}, \varepsilon_{ij})$. In order that (15.18) reduce to (15.16) for uniaxial stress conditions, we define, in complete analogy with plasticity theory, the effective stress σ_{eff} and the *effective creep strain* ε^{cr}_{eff} by

$$\sigma_{eff} = \left(\frac{3}{2}s_{ij}s_{ij}\right)^{1/2}; \quad \varepsilon^{cr}_{eff} = \int_0^t \dot{\varepsilon}^{cr}_{eff}dt; \quad \dot{\varepsilon}^{cr}_{eff} = \left(\frac{2}{3}\dot{\varepsilon}^{cr}_{ij}\dot{\varepsilon}^{cr}_{ij}\right)^{1/2} \tag{15.19}$$

cf. (9.60) and (9.62). The viscosity parameter η is now taken as

$$\eta = \eta(\sigma_{eff}, \varepsilon^{cr}_{eff}) \tag{15.20}$$

Since σ_{eff} and ε^{cr}_{eff} for uniaxial stress conditions reduce to $|\sigma|$ and $|\varepsilon^{cr}|$ respectively, the formulation (15.18) and (15.20) reduces exactly to (15.16) for uniaxial conditions and η becomes

$$\frac{1}{\eta(\sigma_{eff}, \varepsilon^{cr}_{eff})} = \frac{mA^{\frac{1}{m}}}{t^*\sigma^*}\left(\frac{\sigma_{eff}}{\sigma^*}\right)^{\frac{n}{m}-1}(\varepsilon^{cr}_{eff})^{\frac{m-1}{m}} \tag{15.21}$$

Finally, insertion of this expression into (15.18b) and recalling that the elastic stiffness tensor D_{ijkl} is the inverse to the elastic flexibility tensor C_{ijkl}, we obtain the result

Odqvist formulation of power law creep

$$\dot{\sigma}_{ij} = D_{ijkl}(\dot{\varepsilon}_{kl} - \dot{\varepsilon}^{cr}_{kl})$$

where

$$\dot{\varepsilon}^{cr}_{ij} = \frac{mA^{\frac{1}{m}}}{t^*}\left(\frac{\sigma_{eff}}{\sigma^*}\right)^{\frac{n}{m}}\left(\varepsilon^{cr}_{eff}\right)^{\frac{m-1}{m}}\frac{3s_{ij}}{2\sigma_{eff}} \tag{15.22}$$

This generalization to three-dimensional stress states was achieved by Odqvist (1934) although only secondary creep ($m = 1$) was considered. For constant multiaxial stresses, (15.22) is in close agreement with experimental data as discussed by Odqvist and Hult (1962) and Odqvist (1966).

The format (15.22) exhibits strain-hardening and it is tempting to generalize the result in a similar fashion as when the uniaxial formulation (15.11) was generalized to (15.12). We then obtain

$$\dot{\varepsilon}^{cr}_{ij} = \Lambda\frac{3s_{ij}}{2\sigma_{eff}}; \qquad \Lambda = \Lambda(\sigma_{eff}, \varepsilon^{cr}_{eff}) \tag{15.23}$$

where the function Λ with the unit [1/s] is chosen is accordance with experimental data. Further generalizations almost suggest themselves. Considering the von Mises function $f = (\frac{3}{2}s_{ij}s_{ij})^{1/2}$, the above result can be written as $\dot{\varepsilon}^{cr}_{ij} = \Lambda\partial f/\partial\sigma_{ij}$, i.e. f serves as a potential function. The formulation now looks very much like plasticity theory and in that spirit - cf. the discussion in Section 10.1 - the next generalization is to adopt a general potential function $g = g(\sigma_{ij}, K_\alpha)$ where K_α are hardening parameters and then achieve the following general format

General creep formulation

$$\dot{\sigma}_{ij} = D_{ijkl}(\dot{\varepsilon}_{kl} - \dot{\varepsilon}^{cr}_{kl})$$

where

$$\dot{\varepsilon}^{cr}_{ij} = \Lambda\frac{\partial g}{\partial\sigma_{ij}} \tag{15.24}$$

and

$$g(\sigma_{ij}, K_\alpha); \qquad \Lambda = \Lambda(\sigma_{ij}, \kappa_\alpha) \geq 0$$

The function Λ is chosen

Here κ_α are internal variables and K_α are the corresponding hardening parameters, cf. the discussion in Section 10.1. If only one internal variable κ in terms of the effective creep strain ε^{cr}_{eff} is chosen and Λ is taken as $\Lambda = \Lambda(\sigma_{eff}, \varepsilon^{cr}_{eff})$

and $g = (\frac{3}{2}s_{ij}s_{ij})^{1/2}$, then (15.24) reduces to (15.23). In general, evolution laws need to be established for $\dot{K}_\alpha$ and/or $\dot{\kappa}_\alpha$.

The general format (15.24) looks very much like the general plasticity format; however, there are important differences. First of all, no yield criterion is involved in (15.24) and secondly, the function Λ is directly prescribed by us based on experimental evidence. In plasticity theory, we have $\dot{\varepsilon}_{ij}^p = \dot{\lambda}\partial g/\partial\sigma_{ij}$, but here the plastic multiplier $\dot{\lambda}$ is determined as a consequence of the consistency relation. In creep theory, however, there is no yield criterion so the function Λ is directly chosen by us to fit the experimental data in the best possible way.

Moreover, since no yield criterion exists, the question of loading and unloading disappears. Another difference is that whereas development of plastic strains requires a change of stresses or strains, then also for constant stresses, (15.24) shows that a development of creep strains occurs.

Apart from those differences, the similarity between creep theory and plasticity theory is close and in the following we will take full advantage of this fact. As an example, *orthotropic creep theory* is achieved by taking D_{ijkl} to be orthotropic and choosing the potential function g, for instance, as the orthotropic Hill function discussed in Sections 8.13 and 12.6.

15.3.1 Bodner and Partom model

We have shown that the generalized strain-hardening model (15.22) exhibits a number of limitations when larger stress changes occur. Let us therefore turn to the general format (15.24) and investigate other specific possibilities.

As an example, we will discuss the model proposed by Bodner and Partom. A number of other authors has also contributed to the development of this model, but its origins were proposed by Bodner (1968), Bodner and Partom (1972, 1975), Bodner *et al.* (1979) and a comprehensive review is given by Bodner (1987) and Stouffer and Dame (1996).

The term *state variable approach* is occasionally used for the model of Bodner and Partom and some authors even use the notation of a *unified* model. A number of such models exists, for instance Hart (1970), Miller (1976, 1987a,b), Robinson (1978), Walker (1981) and Krempl (1996) and Krempl *et al.* (1986), all of which have been proposed within the last two or three decades; detailed reviews are given by Stouffer and Dame (1996) as well as by Miller (1987a,b) and Krausz and Krausz (1996). These models have been developed to meet the increasing demands within the gas-turbine and nuclear industry to deal with complex thermo-mechanical loadings including creep and cyclic loadings. As a typical example of such models, we will here focus on the Bodner-Partom model.

Within the general framework (15.24), the potential function g is chosen as

$$g = \frac{1}{2} s_{ij} s_{ij} \quad i.e. \quad \dot{\varepsilon}_{ij}^{cr} = \Lambda s_{ij} \tag{15.25}$$

In analogy with the definition $J_2 = \frac{1}{2} s_{ij} s_{ij} = \frac{1}{3} \sigma_{eff}^2$, the invariant D_2 is defined as

$$D_2 = \frac{1}{2} \dot{\varepsilon}_{ij}^{cr} \dot{\varepsilon}_{ij}^{cr}$$

and it appears that $D_2 = \frac{3}{4} (\dot{\varepsilon}_{eff}^{cr})^2$, cf. (15.19). Since $\sqrt{D_2} \sim \dot{\varepsilon}_{eff}^{cr}$, an expression for $\sqrt{D_2}$ is directly postulated based on general experimental evidence, i.e.

Evolution equation

$$\sqrt{D_2} = D_0 e^{-\frac{1}{2}(\frac{Z^2}{\sigma_{eff}^2})^n} \tag{15.26}$$

where D_0 is a positive parameter with the dimension [1/s], Z is a positive variable with the dimension of stress and n is a dimensionless positive parameter. Since $\dot{\varepsilon}_{eff}^{cr}$ can be considered to be the time rate of an internal variable, i.e. $\dot{\kappa}$, so can $\sqrt{D_2}$ and it is then natural to consider Z as a *hardening parameter*. Formally, (15.26) can therefore be viewed as an evolution law in the format $\dot{\kappa} = f(\sigma_{eff}, K)$; in the literature, expression (15.26) is often called the *kinetic equation*. However, what in this situation is termed an internal variable and a hardening parameter is open for discussion and most authors within these state variable models prefer to call Z an internal variable. Since both internal variables and hardening parameters characterize the state of the material, they are *state variables* and the concept is therefore often termed the *state variable approach*, cf. Stouffer and Dame (1996).

Multiply each side of (15.25b) by itself to obtain

$$\Lambda = \frac{\sqrt{3D_2}}{\sigma_{eff}}$$

With (15.26), (15.25b) then takes the form

Bodner-Partom

$$\dot{\varepsilon}_{ij}^{cr} = \Lambda s_{ij}$$

where

$$\Lambda = \Lambda(\sigma_{eff}, Z) = \frac{\sqrt{3} D_0}{\sigma_{eff}} e^{-\frac{1}{2}(\frac{Z^2}{\sigma_{eff}^2})^n} \geq 0 \tag{15.27}$$

Despite the views often put forward in the literature, it is evident that this model is, essentially, a creep model since even constant stresses will result in the development of strains. To evaluate the choice of the evolution law (15.26) - the kinetic equation - and to identify the role of the hardening parameter Z, the expression above is evaluated for uniaxial stress conditions to obtain

$$\dot{\varepsilon}^{cr} = \frac{2D_0}{\sqrt{3}} e^{-\frac{1}{2}\left(\frac{Z^2}{\sigma^2}\right)^n} \tag{15.28}$$

Therefore $2D_0/\sqrt{3}$ is the maximum value of $\dot{\varepsilon}^{cr}$. It also appears that $\dot{\varepsilon}^{cr}$ is a decreasing function of Z^2/σ^2; when $Z^2/\sigma^2 \to \infty$ - which it does for small stresses - then $\dot{\varepsilon}^{cr} \to 0$, as expected, and when $Z^2/\sigma^2 \ll 1$ - i.e. large stresses - then $\dot{\varepsilon}^{cr} \to 2D_0/\sqrt{3}$. Therefore, Z is called in the literature the *equivalent yield stress*, since it is the threshold beyond which the (creep) deformation becomes pronounced. Moreover, the creep strain rate $\dot{\varepsilon}^{cr}$ depends nonlinearly on the stress state and this nonlinearity is controlled by the exponent n. It will be shown later that the smaller the exponent n, the more strain-rate sensitive will be the response of the material.

Consider now a standard creep test and assume that the positive variable Z increases from its initial value and approaches a constant value; then the ratio Z^2/σ^2 will increase and eventually approach a constant value. In turn, the inelastic strain rate $\dot{\varepsilon}^{cr}$ will first be large and then approach a constant, smaller value, but this is exactly what happens in a creep test: First primary creep occurs and eventually secondary creep occurs. The choice (15.26) and thereby (15.28) therefore fulfills all our expectations.

It turns out that a number of phenomena can be modeled, if Z is split into two contributions according to

$$\boxed{\begin{array}{l} Z = Z^I + Z^D \\ \textit{where} \\ Z^I = \textit{isotropic hardening parameter} \\ Z^D = \textit{directional hardening parameter} \end{array}} \tag{15.29}$$

It is not surprising that the *isotropic hardening parameter* Z^I will depend on some scalar quantities whereas the so-called *directional hardening parameter* Z^D must depend on some second-order tensor much along the lines of kinematic hardening in plasticity.

The next topic is to choose an evolution law for $\dot{Z}$ such that it fulfills the requirements established above: in a creep test, the positive quantity Z should increase from its initial value and eventually reach a constant value. Let us for the time being ignore the influence of the directional hardening parameter Z^D and establish the evolution law for $\dot{Z}^I$. What can create a change in Z^I is development of creep strains, so one possibility would be to relate $\dot{Z}^I$ to $\dot{\varepsilon}^{cr}_{eff}$ (or $\sqrt{D_2}$). However, another non-negative quantity is the rate of inelastic

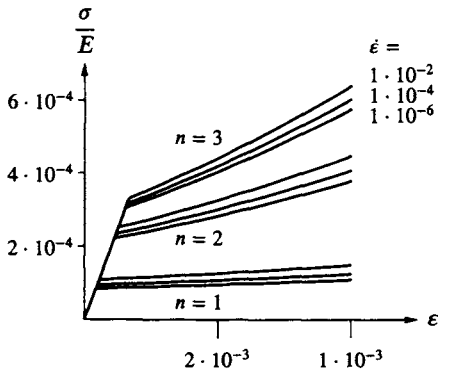

Figure 15.8: Constant strain-rate tests predicted by (15.30) for different values of the exponent n; material parameters: $m_1 E = 3.4 \cdot 10^5$, $D_0 = 10^4\,[1/s]$, $Z_0/E = 5.8 \cdot 10^{-4}$ and $Z_1/E = 3.3 \cdot 10^{-3}$ which are representative for aluminum at $200\,°C$ where also $n = 1.43$ holds, cf. Bodner (1987).

work $\dot{W}^{cr} = \sigma_{ij}\dot{\epsilon}^{cr}_{ij}$, which according to (15.27) becomes $\dot{W}^{cr} = \Lambda s_{ij}s_{ij} \geq 0$. A simple evolution law would then be $\dot{Z}^I = (m_1 Z_1)\dot{W}^{cr}$ where $m_1 Z_1$ is a positive material parameter (the reason for this somewhat curious notation for one material parameter will become apparent in a moment); however, since $\dot{W}^{cr} > 0$ for all non-zero stresses, the result is that Z^I increases without bounds and then only primary creep in a creep test can be modeled. To eventually obtain secondary creep in a creep test, it is required that Z^I eventually reach a constant value. This can be achieved by writing the evolution law as

$$\dot{Z}^I = m_1 Z_1 \dot{W}^{cr} - \underbrace{m_1 Z^I \dot{W}^{cr}}_{\text{dynamic recovery term}} = m_1(Z_1 - Z^I)\dot{W}^{cr} \tag{15.30}$$

where

$$\boxed{\begin{array}{l} Z_1 = \textit{saturation value of } Z^I;\quad Z_0 = \textit{initial value of } Z^I \\ 0 < Z_0 \leq Z^I \leq Z_1 \end{array}}$$

and m_1 [1/Pa], Z_0 [Pa] and Z_1 [Pa] are positive material parameters. It appears that $\dot{Z}^I > 0$ holds in the beginning until Z^I eventually reaches the value Z_1 and then $\dot{Z}^I = 0$ whereby secondary creep is encountered in a creep test. The parameter Z_1 is therefore called the *saturation value* of Z^I and the second term on the right-hand side of (15.30) is called the *dynamic recovery term.*

For uniaxial tension, the predictions of (15.27) and (15.30) for constant strain-rate tests are shown in Fig. 15.8 where the material data are representative for aluminum at 200 °C and also $n = 1.43$ is representative. As already mentioned, the smaller the n exponent, the larger the strain-rate sensitivity of the

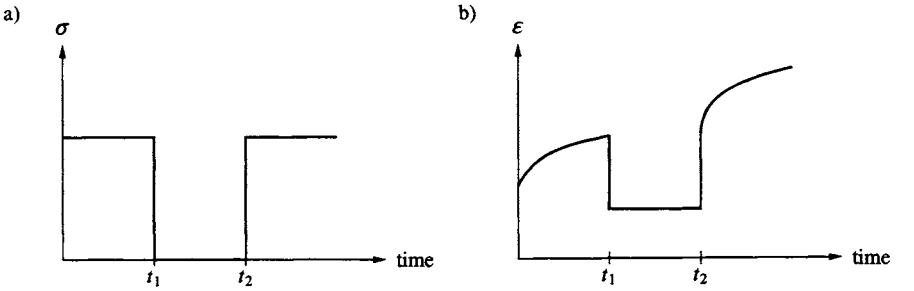

Figure 15.9: Interrupted creep test. Secondary creep is assumed to occur at time $t = t_1$, but reloading at time $t = t_2$ introduces primary creep.

material. Moreover, it is also seen that the material behaves as if there were a yield stress below which insignificant creep strains develop; this apparent yield stress increases with the exponent n.

To be able to model a realistic response for stress changes like those shown in Figs. 15.5-15.7, an additional term is introduced into the evolution law (15.30), which now takes the form

Evolution law for isotropic hardening parameter

$$\dot{Z}^I = m_1(Z_1 - Z^I)\dot{W}^{cr} - \underbrace{A_1 Z_1 \left(\frac{Z^I - Z_2}{Z_1}\right)^{r_1}}_{\text{thermal recovery term}} \tag{15.31}$$

where $0 \leq Z_0 \leq Z^I \leq Z_1$ *and* $Z_2 = Z_0$

where the additional positive material parameters have the dimensions A_1 [1/s], Z_2 [Pa] and r_1 is dimensionless. In Bodner (1987), for instance, Z_2 is recommended to be chosen close to Z_0, but here we require $Z_2 = Z_0$. Since the exponent r_1 can be any positive number, the thermal recovery term only makes sense if $Z_0 \geq Z_2$, but if $Z_0 > Z_2$ holds then (15.31) will predict $\dot{Z}^i < 0$ even before any load is applied and to avoid this awkward situation, it is here required that $Z_2 = Z_0$.

To illustrate the influence of the *thermal recovery term* in (15.31), consider the interrupted creep test in Fig. 15.9. For simplicity, it is assumed that secondary creep has been achieved at time $t = t_1$. During the unloaded period, $\dot{W}^{cr} = 0$ holds and (15.31) then predicts $\dot{Z}^I < 0$, that is, Z^I is decreased from its value in the secondary creep regime towards a smaller Z^I-value, i.e towards the primary creep regime. Therefore, when reloaded at time $t = t_2$ primary creep is introduced and this is exactly the behavior strived for, cf. Fig. 15.6.

The thermal recovery term is occasionally termed the *static* recovery term since it is active even during unloaded periods in contrast to the dynamic recovery term that is only active when the material is loaded.

To improve the response during cyclic loading, the directional hardening parameter Z^D is introduced, cf. (15.29). To establish the evolution law for $\dot{Z}^D$, a symmetric stress tensor β_{ij} is introduced, much along the lines of a back-stress tensor for kinematic hardening in plasticity theory. The following definitions are introduced

$$u_{ij} = \frac{\sigma_{ij}}{\sqrt{\sigma_{kl}\sigma_{kl}}}; \quad v_{ij} = \frac{\beta_{ij}}{\sqrt{\beta_{kl}\beta_{kl}}}$$

and

$$Z^D = \beta_{ij}u_{ij}$$

where $\beta_{ij}(t=0) = 0$

i.e. u_{ij} is the normalized stress tensor and v_{ij} is the normalized β_{ij}-tensor.

In complete analogy with (15.31), the following evolution law for $\dot{\beta}_{ij}$ is adopted

$$\dot{\beta}_{ij} = m_2(Z_3 u_{ij} - \beta_{ij})\dot{W}^{cr} - A_2 Z_1 \left(\frac{\sqrt{\beta_{kl}\beta_{kl}}}{Z_1}\right)^{r_2} v_{ij} \tag{15.32}$$

where m_2 [1/Pa], Z_3 [Pa], A_2 [1/s] and r_2 (dimensionless) are additional positive material parameters. The evolution law for $\dot{Z}^D$ is then determined by $\dot{Z}^D = \dot{\beta}_{ij}u_{ij} + \beta_{ij}\dot{u}_{ij}$. Similar to (15.31), the term $m_2\beta_{ij}\dot{W}^{cr}$ is called a dynamic recovery term and the last term on the right-hand side is called a thermal recovery term.

The directional hardening parameter Z^D improves the response during cyclic loading, for a the detailed discussion of (15.31) the reader is referred to, for instance Bodner (1987), for a further evaluation and comparison with experimental data. It is of interest to note that (15.32) is similar in structure to (15.31) and a fundamental similarity exists also between (15.32) and the Armstrong-Frederick evolution law cf. (13.70).

We have seen that the Bodner-Partom model contains a number of interesting features. However, the number of material parameters is large and the identification of these parameters from experimental data is not trivial; a discussion is given by Bodner (1987) and Rowley and Thornton (1996).

15.4 Viscoplasticity

We will now turn our interest to *viscoplasticity*, which has received considerable attention during the last decades, and also refer to the comprehensive reviews presented by Perzyna (1966, 1971), Lemaitre and Chaboche (1990), Lubliner (1990), Krausz and Krausz (1996) as well as Simo and Hughes (1998). In the beginning of the 20th century, where the basic concepts for linear viscoelasticity and viscous fluids were known, it was observed that some viscous materials

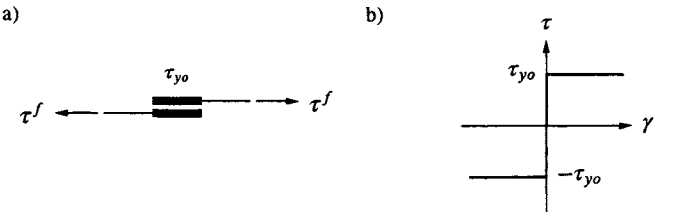

Figure 15.10: a) Saint-Venant friction element, b) response.

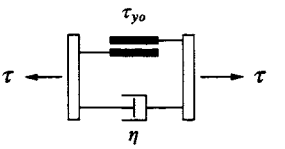

Figure 15.11: Bingham model.

could not be categorized into these two groups of materials. For instance, a large drop of oil-paint will run down the wall whereas a small drop will remain its position on the wall; it follows that a certain amount of stress is required in order that the material exhibits viscous effects.

To model this behavior, we first introduce the *friction element* shown in Fig. 15.10 where superscript 'f' refers to 'frictional'; traditionally, this friction element is attributed to Saint-Venant. If a shear stress τ^f is applied, the friction element behaves as a rigid body when $|\tau^f| < \tau_{yo}$ where τ_{yo} is the *yield shear stress*; development of a shear strain γ is only possible if $|\tau^f| = \tau_{yo}$. The constitutive model for the friction element is therefore

$$\dot{\gamma}^f = 0 \quad \text{if} \quad |\tau^f| < \tau_{yo}$$
$$\dot{\gamma}^f \geq 0 \quad \text{if} \quad \tau^f = \tau_{yo}$$
$$\dot{\gamma}^f \leq 0 \quad \text{if} \quad \tau^f = -\tau_{yo}$$

and deformations are only possible if the shear stress equals the yield shear stress.

To model the oil-paint behavior mentioned above, Bingham (1922) introduced the rigid-viscous model shown in Fig. 15.11. This *Bingham model* consists of a friction element and a viscous element in parallel. In accordance with (14.5) the constitutive law for the viscous element is $\dot{\gamma}^v = \tau^v/\eta$ where η is a viscosity parameter. To establish the constitutive law for the Bingham model, we first observe that $\tau = \tau^f + \tau^v$ and $\dot{\gamma} = \dot{\gamma}^f = \dot{\gamma}^v$. If $|\tau^f| < \tau_{yo}$ then $\dot{\gamma}^f = 0$ i.e. $\dot{\gamma} = 0$ and then $\tau^v = 0$ and thereby $|\tau| < \tau_{yo}$. If $\tau^f = \tau_{yo}$ then $\dot{\gamma}^f = \dot{\gamma} = \tau^v/\eta \geq 0$ and as $\tau^v = \tau - \tau^f = \tau - \tau_{yo} \geq 0$ we obtain $\tau \geq \tau_{yo}$ and

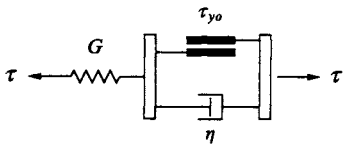

Figure 15.12: Hencky model consisting of a Bingham element and an elastic spring in series.

$\dot{\gamma} = (\tau - \tau_{yo})/\eta = (1 - \frac{\tau_{yo}}{\tau})\frac{\tau}{\eta}$. Similar considerations hold if $\tau^f = -\tau_{yo}$ and in conclusion, we obtain

$$\boxed{\begin{array}{lll} \dot{\gamma} = 0 & \text{if} & |\tau| \le \tau_{yo} \\ \dot{\gamma} = \dfrac{1 - \frac{\tau_{yo}}{|\tau|}}{\eta}\tau & \text{if} & |\tau| \ge \tau_{yo} \end{array} \quad \textit{Bingham}}$$

Therefore if $|\tau| \le \tau_{yo}$ the Bingham element is rigid and if $|\tau| > \tau_{yo}$ the element exhibits secondary creep.

The *Hencky model* shown in Fig. 15.12 comprises a Bingham model and an elastic spring in series, Hencky (1925); the elastic spring is characterized by the shear modulus G. To establish the constitutive law, it is observed that $\tau = \tau^e = \tau^B$ and $\dot{\gamma} = \dot{\gamma}^e + \dot{\gamma}^B$ and it then follows that

$$\begin{aligned} \dot{\gamma} &= \frac{\dot{\tau}}{G} && \text{if} \quad |\tau| \le \tau_{yo} \\ \dot{\gamma} &= \frac{\dot{\tau}}{G} + \frac{1 - \frac{\tau_{yo}}{|\tau|}}{\eta}\tau && \text{if} \quad |\tau| \ge \tau_{yo} \end{aligned} \tag{15.33}$$

The response of the Hencky model in a creep test is shown in Fig. 15.13. If the shear stress is below the yield shear stress τ_{yo}, the material is elastic and no creep strains develop whereas secondary creep occurs if $\tau > \tau_{yo}$.

To generalize the Hencky format (15.33) to isotropic three-dimensional behavior, it is first observed that the viscous strains might be thought of as being fluid-like, i.e. incompressible and it then follows that $\dot{\epsilon}_{kk} = \dot{\sigma}_{kk}/3K$, where K is the bulk modulus. It is also observed that $J_2 = \frac{1}{2}s_{ij}s_{ij}$ for pure shear reduces to $\sqrt{J_2} = |\tau|$ and that the engineering shear strains are twice the tensorial shear strains; then an immediate generalization of (15.33) becomes

$$\begin{aligned} \dot{\epsilon}_{ii} &= \frac{\dot{\sigma}_{ii}}{3K} \\ \dot{e}_{ij} &= \frac{\dot{s}_{ij}}{2G} && \text{if} \quad \sqrt{J_2} \le \tau_{yo} \\ \dot{e}_{ij} &= \frac{\dot{s}_{ij}}{2G} + \frac{1 - \frac{\tau_{yo}}{\sqrt{J_2}}}{2\eta}s_{ij} && \text{if} \quad \sqrt{J_2} \ge \tau_{yo} \end{aligned}$$

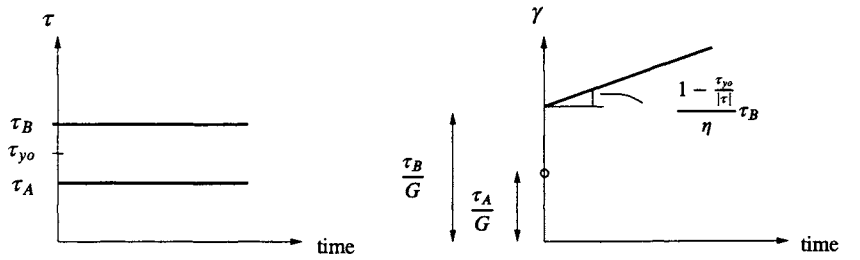

Figure 15.13: Creep test of Hencky model; one test below the yield shear stress τ_{yo} and another above τ_{yo}.

This generalization was established by Hohenemser and Prager (1932) and if the elastic response is disregarded, the formulation was given already by Hencky (1925). Observing that $\sqrt{3J_2} = \sigma_{eff}$ and that according to the yield criterion of von Mises, the initial yield stress σ_{yo} in tension is given by $\sigma_{yo} = \sqrt{3}\tau_{yo}$, the format above can also be written as

Hohenemser-Prager viscoplasticity

$$\dot{\varepsilon}_{ij} = \dot{\varepsilon}^e_{ij} + \dot{\varepsilon}^{vp}_{ij}$$

where

$$\dot{\varepsilon}^e_{ij} = C_{ijkl}\dot{\sigma}_{kl}$$

$$\dot{\varepsilon}^{vp}_{ij} = 0 \qquad \text{if} \quad \sigma_{eff} \leq \sigma_{yo}$$

$$\dot{\varepsilon}^{vp}_{ij} = \frac{1 - \frac{\sigma_{yo}}{\sigma_{eff}}}{2\eta} s_{ij} \qquad \text{if} \quad \sigma_{eff} \geq \sigma_{yo} \tag{15.34}$$

It follows that when the stress state is inside or on the initial yield surface $F(\sigma_{ij}) = \sigma_{eff} - \sigma_{yo} = 0$, i.e. $F(\sigma_{ij}) \leq 0$ an elastic response occurs and if $F(\sigma_{ij}) > 0$ holds viscoplastic strains develop; it is the *excess stress* or the *overstress* $\sigma_{eff} - \sigma_{yo}$ that drives the viscoplastic development. For proportional loading, we also observe that (15.34) implies that the viscoplastic strain rates increase linearly with the stresses.

Following Hohenemser and Prager (1932) an interesting limit process will now be considered. If the viscosity parameter $\eta \to 0$ then, in order that $\dot{\varepsilon}^{vp}_{ij}$ be a finite quantity, we must have $1 - \frac{\sigma_{yo}}{\sigma_{eff}} \to 0$. In that case the factor $(1 - \frac{\sigma_{yo}}{\sigma_{eff}})/\eta \to 0/0 = \dot{\lambda}$ where $\dot{\lambda}$ is an undetermined quantity; therefore when $\eta \to 0$, (15.34) shows that $\dot{\varepsilon}^{vp}_{ij} \to \dot{\lambda} s_{ij}$ i.e. the classical Prandl-Reuss equations, cf. (9.31), where $\dot{\lambda}$ is the plastic multiplier and $\dot{\varepsilon}^{vp}_{ij}$ then becomes the plastic strain rates $\dot{\varepsilon}^{p}_{ij}$.

15.4.1 Perzyna viscoplasticity

Despite these early achievements, viscoplasticity played a minor role for a number of years and it was first when impact phenomena became an area of intensive research that the interest in viscoplasticity was revived. Constant strain-rate tests for a nickel alloy and concrete are displayed in Fig. 15.14 and it appears that the response fits into a viscoplastic framework; below a certain threshold value, the response is linear elastic and above this threshold strain-rate effects occur (note that it is allowable to choose the σ_{yo}-value as any threshold value and not just as the initial yield stress).

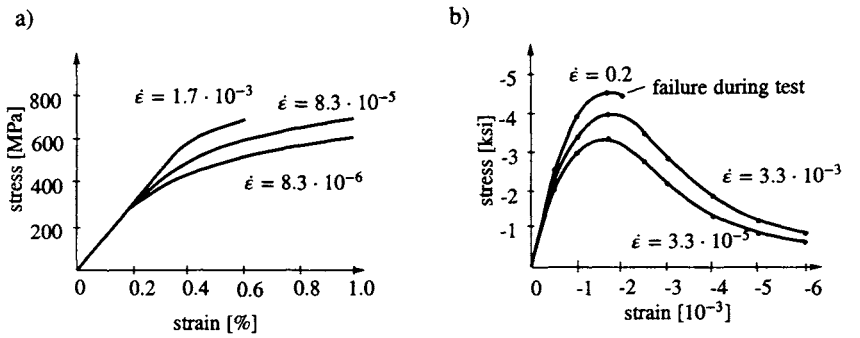

Figure 15.14: Constant strain-rate tests for uniaxial loading; a) nickel-based superalloy, B1900+Hf at 871°C , Chan *et al.* (1988), b) concrete in compression, Dilger *et al.* (1984).

The hardening effects shown in Fig. 15.14 cannot be modeled by the Hohenemser-Prager formulation (15.34) and in this model, the viscoplastic strain rate even depends linearly on strains. For uniaxial tension, Malvern (1951) suggested a model where hardening effects are considered. However, ignoring for the time being hardening effects, it is evident that (15.34) can be reformulated such that the viscoplastic strain rate depends nonlinearly on the stresses. We obtain

$$\dot{\varepsilon}_{ij}^{vp} = \begin{cases} 0 & \text{if } \sigma_{eff} \leq \sigma_{yo} \\ \dfrac{\Phi(F(\sigma_{ij}))}{\eta} \dfrac{3s_{ij}}{2\sigma_{eff}} & \text{if } \sigma_{eff} \geq \sigma_{yo} \end{cases}$$

where the function $\Phi(F(\sigma_{ij}) \geq 0$ is non-negative and $F(\sigma_{ij}) = \sigma_{eff} - \sigma_{yo}$. Moreover, since $\partial F/\partial \sigma_{ij} = 3s_{ij}/(2\sigma_{eff})$ the expression above can be written as

$$\dot{\varepsilon}_{ij}^{vp} = \begin{cases} 0 & \text{if } \sigma_{eff} \leq \sigma_{yo} \\ \dfrac{\Phi(F(\sigma_{ij}))}{\eta} \dfrac{\partial F}{\partial \sigma_{ij}} & \text{if } \sigma_{eff} \geq \sigma_{yo} \end{cases} \tag{15.35}$$

The function $\Phi(F)$ is assumed to be an increasing function of F and it is required that $\Phi(F = 0) = 0$. The formulation (15.35) was presented by Perzyna

(1963). Originally, $F(\sigma_{ij})$ was the yield function according to ideal von Mises plasticity, but we may also consider $F(\sigma_{ij})$ to be the yield function for ideal plasticity in general. With this format, it is easy to generalize so that hardening effects are included. Instead of the expression $F(\sigma_{ij})$ for the initial yield function, we use the expression $f(\sigma_{ij}, K_\alpha)$ for the current yield function, cf. the discussion related to (9.8). One may also allow for a nonassociated formulation and introduce the potential function $g = g(\sigma_{ij}, K_\alpha)$. We are then led to

Perzyna nonassociated viscoplasticity

$$\sigma_{ij} = D_{ijkl}(\varepsilon_{kl} - \varepsilon_{kl}^{vp})$$

$$\dot{\varepsilon}_{ij}^{vp} = \begin{cases} 0 & \text{if } f(\sigma_{ij}, K_\alpha) \leq 0 \\ \dfrac{\Phi(f)}{\eta}\dfrac{\partial g}{\partial \sigma_{ij}} & \text{if } f(\sigma_{ij}, K_\alpha) > 0 \end{cases} \tag{15.36}$$

where $f = f(\sigma_{ij}, K_\alpha) = 0$ *is the static yield surface*

and $\Phi(f) \geq 0$ *as well as* $\Phi(f = 0) = 0$

Moreover, $g = g(\sigma_{ij}, K_\alpha)$ *is the potential function*

Associated viscoplasticity is obtained by choosing the potential function as the yield function, i.e. $g = f(\sigma_{ij}, K_\alpha)$. Then (15.36) takes the format suggested by Perzyna (1966, 1971). In the present context, the surface described by $f(\sigma_{ij}, K_\alpha) = 0$ is called the *static yield surface* and we will return to that aspect in a moment.

Evidently, close similarities exist between Perzyna viscoplasticity and the time-independent plasticity theory discussed in Section 10.1. However, in the Perzyna viscoplasticity the factor $\Phi(f)/\eta$ is chosen by us whereas the corresponding factor in plasticity theory is the plastic multiplier $\dot{\lambda}$ which is determined by the consistency relation. In Perzyna viscoplasticity, the stress state is required to be located outside the static yield surface $f(\sigma_{ij}, K_\alpha)$ in order that viscoplastic strains develop whereas in time-independent plasticity the stresses can never be located outside the yield surface.

With this discussion of the similarities between viscoplasticity and plasticity in mind, we return to the general Perzyna formulation (15.36) and observe that hardening parameters K_α are involved. In analogy with plasticity theory we associate to the hardening parameters K_α some internal variables κ_α and, in general, we have the evolution equations

Evolution equations

$$K_\alpha = K_\alpha(\kappa_\beta)$$

$$\dot{\kappa}_\alpha = -\frac{\Phi(f)}{\eta}\frac{\partial g}{\partial K_\alpha} \tag{15.37}$$

A comparison of the evolution laws for $\dot{\varepsilon}_{ij}^{vp}$ and $\dot{\kappa}_\alpha$ given by (15.36) and (15.37)

with the corresponding evolution laws for $\dot{\varepsilon}_{ij}^{p}$ and $\dot{\kappa}_\alpha$ given by (10.14) underlines the similarities and we refer to (10.14) for a further discussion.

In analogy with the discussion following (15.34), we observe from (15.36) that if the viscosity parameter $\eta \to 0$ then - in order that $\dot{\varepsilon}_{ij}^{vp}$ be a finite quantity - we must have $\Phi(f) \to 0$, i.e. $f \to 0$. As a result $\Phi(f)/\eta \to 0/0 = \dot{\lambda}$ where $\dot{\lambda}$ is an undetermined quantity and we then obtain $\dot{\varepsilon}_{ij}^{vp} \to \dot{\lambda}\partial g/\partial\sigma_{ij}$, i.e. rate independent plasticity theory with $\dot{\lambda}$ being the plastic multiplier

When the viscosity parameter $\eta \to 0$, Perzyna viscoplasticity reduces to rate independent plasticity theory

This property is by Simo and Honein (1990) called the *viscoplastic regularization*

As a further illustration of Perzyna viscoplasticity, assume that the static yield function is taken as isotropic linear hardening of a von Mises material, i.e.

$$f(\sigma_{ij}, K_\alpha) = \sigma_{eff} - \sigma_{yo} - H\varepsilon_{eff}^{vp}$$

where H is a constant. In analogy with the definition of the effective plastic strain, we define the effective viscoplastic strain according to

$$\dot{\varepsilon}_{eff}^{vp} = (\frac{2}{3}\dot{\varepsilon}_{ij}^{vp}\dot{\varepsilon}_{ij}^{vp})^{1/2}; \quad \varepsilon_{eff}^{vp} = \int_0^t \dot{\varepsilon}_{eff}^{vp} dt \tag{15.38}$$

For uniaxial tension, we then obtain

$$\dot{\varepsilon}^{vp} = \begin{cases} 0 & \text{if } f=\sigma-\sigma_{yo}-H\varepsilon^{vp} \le 0 \\ \dfrac{\Phi(f)}{\eta} & \text{if } f=\sigma-\sigma_{yo}-H\varepsilon^{vp} \ge 0 \end{cases}$$

where $\Phi(f) \ge 0$.

A creep test with the constant stress $\sigma_A > \sigma_{yo}$ is shown in Fig. 15.15a). At point A, the overstress is given by $f_A = \sigma_{eff} - \sigma_{yo} - H\varepsilon^{vp} = \sigma_A - \sigma_{yo} > 0$ and we then have $\dot{\varepsilon}^{vp} > 0$. At point B, the overstress has been reduced to $f_B = \sigma_A - \sigma_{yo} - H\varepsilon_B^{vp} > 0$ and $f_B < f_A$ and thereby $\dot{\varepsilon}_B^{vp} < \dot{\varepsilon}_A^{vp}$. Finally, at point C where $f_C = \sigma_A - \sigma_{yo} - H\varepsilon_C^{vp} = 0$, the overstress has been reduced to zero and we have then reached the static yield surface and no more viscoplastic strains develop. The corresponding development over time of the viscoplastic strain is displayed in Fig. 15.15b) and it appears that the material only exhibits primary creep.

It is evident that the conclusions above can be generalized and we obtain

When $t \to \infty$, the stress state is located on the static yield surface

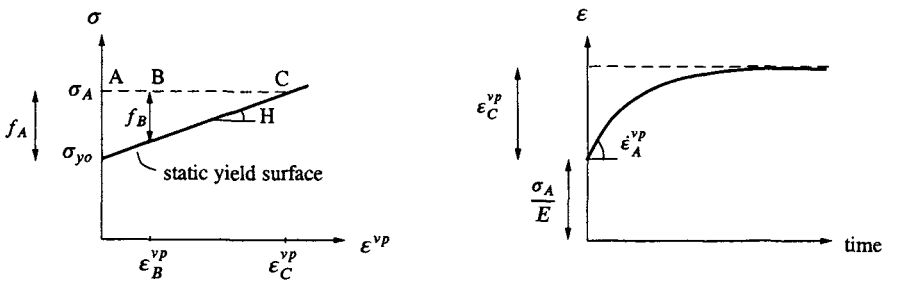

Figure 15.15: Creep test of linear hardening von Mises material; a) illustration in $\sigma-\varepsilon^{vp}$ diagram, b) development of strain over time.

This does not necessarily mean that the solution to a viscoplastic problem for $t \to \infty$ will become identical to the similar problem for plasticity. In the general case, hardening parameters K_α are involved and their development certainly depends on the loading history, and this implies that the solution to the viscoplastic problem and the corresponding plastic problem might differ. However, if the viscoplastic body is loaded by forces that increase infinitely slowly then the viscoplastic solution and the plastic solution coincide, i.e.

If the external loading is applied infinitely slowly, the viscoplastic solution and the plastic solution coincide

Another extreme situation occurs if the load is applied very rapidly. The viscoplastic strain rate will then be large, but the integration of the viscoplastic strain rate over the time duration will be small when the time duration is short. Consequently, the viscoplastic material will in the limit behave as a linear elastic body when the loading rate is large.

In (15.36) the static yield surface $f(\sigma_{ij}, K_\alpha) = 0$ needs not be the same yield surface as that encountered in plasticity theory. Indeed, it is allowable in (15.36) to choose the static yield function such that $f(\sigma_{ij}, K_\alpha) \geq 0$ always; in a von Mises context one might for instance choose the static yield function as $f = \sigma_{eff}$ which implies $f \geq 0$ always. If this choice is adopted and if the factor $\Phi(f)/\eta$ in (15.36) is renamed and called Λ then the Perzyna format reduces to the general creep format (15.24); therefore

If the static yield function $f(\sigma_{ij}, K_\alpha)$ in Perzyna viscoplasticity is chosen as $f(\sigma_{ij}, K_\alpha) \geq 0$ then Perzyna viscoplasticity reduces to general creep theory

It follows that Perzyna viscoplasticity contains two interesting bounds: if the time goes towards infinity, the stresses will be located on the static yield surface and if the static yield function is chosen properly, general creep theory emerges.

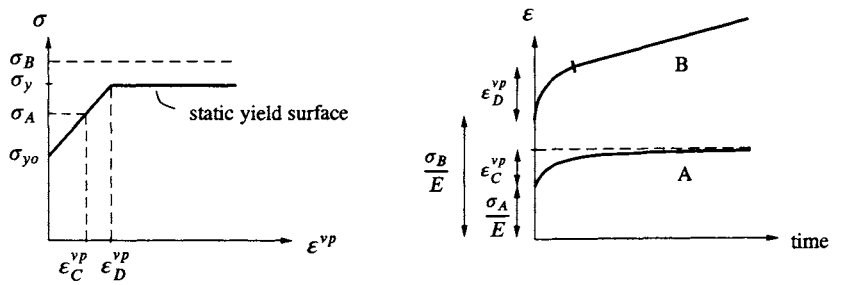

Figure 15.16: Creep tests showing both primary creep and secondary creep; a) primary creep, b) primary creep followed by stationary creep.

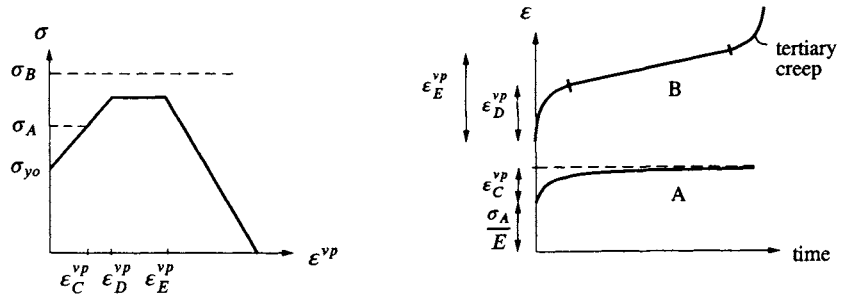

Figure 15.17: Creep tests showing primary, secondary and tertiary creep; a) primary creep, b) primary creep followed by secondary creep and tertiary creep.

Let us also illustrate that by proper choice of the static yield surface, a number of different creep characteristics can be modeled. Suppose the static yield function is chosen as shown in Fig. 15.16a) where ideal plasticity is reached with the yield stress σ_y when the viscoplastic strain has increased to the value ε_D^{vp}. For the constant stress σ_A, which is below σ_y, only primary creep is activated just like in Fig. 15.15. However, for the constant stress σ_B, which is larger than the yield stress σ_y, we first have development of primary creep and then - after some time - when the distance between the current stress and the static yield curve is constant, secondary creep develops.

In Fig. 15.17 the static yield surface is chosen such that it involves a softening branch when the viscoplastic strain is larger that ε_E^{vp}. As before, the constant stress σ_A will only give rise to primary creep, but the constant stress σ_B will first activate primary creep, then secondary creep and eventually tertiary creep, which might even involve creep failure.

Let us generalize these ideas and take the rate of the static yield function to

obtain

$$\dot{f} = \frac{\partial f}{\partial \sigma_{ij}} \dot{\sigma}_{ij} + \frac{\partial f}{\partial K_\beta} \dot{K}_\beta$$

which with (15.37) becomes

$$\dot{f} = \frac{\partial f}{\partial \sigma_{ij}} \dot{\sigma}_{ij} - \frac{\partial f}{\partial K_\beta} \frac{\partial K_\beta}{\partial \kappa_\alpha} \frac{\partial g}{\partial K_\alpha} \frac{\Phi(f)}{\eta} \tag{15.39}$$

In analogy with (10.17) and (10.13) we define the generalized plastic modulus H as

$$\boxed{H = \frac{\partial f}{\partial K_\beta} \frac{\partial K_\beta}{\partial \kappa_\alpha} \frac{\partial g}{\partial K_\alpha}}$$

that is, (15.39) becomes

$$\dot{f} = \frac{\partial f}{\partial \sigma_{ij}} \dot{\sigma}_{ij} - H \frac{\Phi(f)}{\eta}$$

In a creep test, the stresses are constant and we then have $\dot{f} = -H\Phi(f)/\eta$. If $H > 0$ then $\dot{f} < 0$, i.e. primary creep, if $H = 0$ then $\dot{f} = 0$ and secondary creep develops and, finally, if $H < 0$ then $\dot{f} > 0$ and tertiary creep is present. Consequently

$$\boxed{\begin{array}{l} H > 0 \Rightarrow \textit{hardening viscoplasticity (primary creep)} \\ H = 0 \Rightarrow \textit{ideal viscoplasticity (secondary creep)} \\ H < 0 \Rightarrow \textit{softening viscoplasticity (tertiary creep)} \end{array}}$$

and these conclusions correspond to those applicable in plasticity theory, cf. (10.33); further discussions are given by Lubliner (1990) as well as by Ristinmaa and Ottosen (2000).

We will now reformulate the Perzyna equations (15.36) in a manner which leads to the interesting concept of a *dynamic yield surface* introduced by Perzyna (1963, 1966). Use of (15.36) in expression (15.38) for the effective viscoplastic strain rate provides

$$\eta \dot{\varepsilon}^{vp}_{eff} \sqrt{\frac{2}{3} \frac{\partial g}{\partial \sigma_{ij}} \frac{\partial g}{\partial \sigma_{ij}}} = \Phi(f) \tag{15.40}$$

Associated with the non-negative monotonic increasing function Φ there exists an inverse non-negative function φ with the properties

$$\boxed{\varphi(\Phi(f)) = f \quad \textit{i.e.} \quad \varphi \geq 0 \ \textit{and} \ \varphi(0) = 0} \tag{15.41}$$

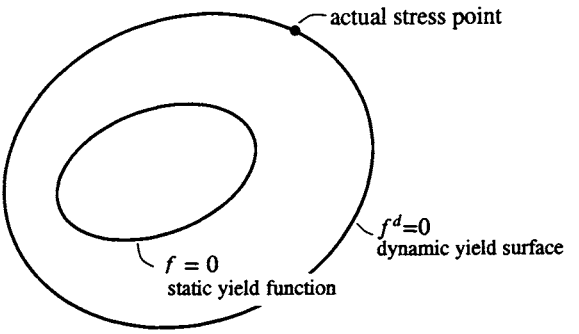

Figure 15.18: Illustration of static and dynamic yield surfaces.

The property $\phi(0) = 0$ follows directly from the previous mentioned requirement $\Phi(0) = 0$. We then obtain from (15.40)

$$\varphi(\eta\dot{\varepsilon}^{vp}_{eff}\sqrt{\frac{2}{3}\frac{\partial g}{\partial\sigma_{ij}}\frac{\partial g}{\partial\sigma_{ij}}}) = f \tag{15.42}$$

Define the dynamic yield surface f^d by $f^d = f - \varphi$. It then follows from (15.42) that $f^d = 0$ holds during viscoplastic development. If the response is elastic then $f < 0$ as well as $\dot{\varepsilon}^{vp}_{eff} = 0$ implying that $f^d = f - \varphi = f < 0$. We also observe that $f^d > 0$ can never occur. In conclusion

Dynamic yield function

$$f^d = f - \varphi$$

$$f^d \begin{cases} < 0 & \textit{elastic response} \\ = 0 & \textit{viscoplastic response} \end{cases}$$

f = *static yield function*

$$\varphi = \varphi(\eta\dot{\varepsilon}^{vp}_{eff}\sqrt{\frac{2}{3}\frac{\partial g}{\partial\sigma_{ij}}\frac{\partial g}{\partial\sigma_{ij}}})$$

(15.43)

This result is illustrated in Fig. 15.18 and a further discussion is provided by Ristinmaa and Ottosen (2000).

To illustrate this concept, assume that the static yield function is taken as an isotropic hardening von Mises formulation, i.e.

$$f = \sigma_{eff} - \sigma_{yo} - K(\kappa) \tag{15.44}$$

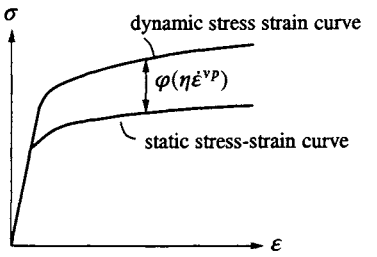

Figure 15.19: Static and dynamic stress-strain curves according to (15.47).

Then (15.36) gives

$$\dot{\varepsilon}_{ij}^{vp} = \frac{\Phi(f)}{\eta}\frac{3s_{ij}}{2\sigma_{eff}} \tag{15.45}$$

and the effective viscoplastic strain rate defined by (15.38) becomes

$$\dot{\varepsilon}_{eff}^{vp} = \frac{\Phi(f)}{\eta} \tag{15.46}$$

Use of the inverse function φ defined by (15.41) leads to

$$\varphi(\eta\dot{\varepsilon}_{eff}^{vp}) = f$$

The dynamic yield function is then given by $f^d = f - \varphi(\eta\dot{\varepsilon}_{eff}^{vp}) = 0$ which with (15.44) gives

$$\sigma_{eff} = \sigma_{yo} + K(\varepsilon_{eff}^{vp}) + \varphi(\eta\dot{\varepsilon}_{eff}^{vp}) \tag{15.47}$$

where the internal variable κ was chosen as $\kappa = \varepsilon_{eff}^{vp}$. The above expression has the uniaxial interpretation shown in Fig. 15.19.

Indeed, (15.47) makes for some interesting interpretations of various experimental findings. For steel and metals, it is observed experimentally that the initial yield stress increases with the loading rate as shown in Fig. 15.20 where the experimental data are taken from Manjoine (1944).

To fit such data, the model of Cowper and Symonds (1962) is often adopted; this model reads

$$\sigma_{yo}^{d} = \sigma_{yo}[1 + (\frac{\dot{\varepsilon}_{eff}^{vp}}{D})^{1/p}] \tag{15.48}$$

where σ_{yo}^{d} is the dynamic initial yield stress and σ_{yo}, as usual, is the static initial yield stress. Moreover, D is an arbitrary, positive reference strain rate with the sole purpose of making the term $\dot{\varepsilon}_{eff}^{vp}/D$ dimensionless; evidently when

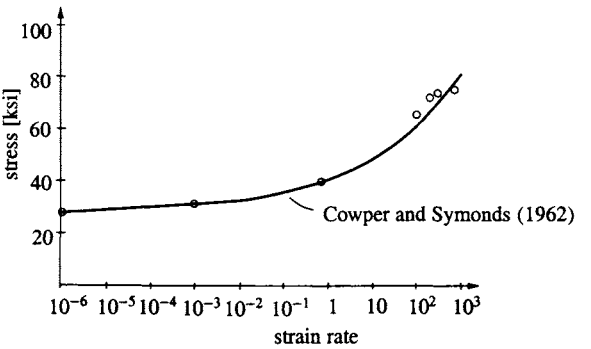

Figure 15.20: Variation of initial yield stress for mild steel with loading rate, Manjoine (1944). Curve fitting of Cowper-Symonds model (15.48) with $D = 30$ [1/s] and $p = 5$.

$\dot{\varepsilon}_{eff}^{vp} = D$ then $\sigma_{yo}^{d} = 2\sigma_{yo}$. The positive dimensionless parameter p in (15.48) is often in the range of 5-10. It is emphasized that the strain rate used in (15.48) is the effective viscoplastic strain rate and not the total strain rate as used by some authors.

Evaluation of (15.47) at initiation of viscoplasticity and by using $K(0) = 0$ give $\sigma_{eff} = \sigma_{yo} + \varphi(\eta\dot{\varepsilon}_{eff}^{vp})$. A comparison with (15.48) then provides

$$\varphi(\eta\dot{\varepsilon}_{eff}^{vp}) = \sigma_{yo}\left(\frac{\dot{\varepsilon}_{eff}^{vp}}{D}\right)^{1/p}$$

which can be written as

$$\varphi(x) = \sigma_{yo}\left(\frac{x}{\eta D}\right)^{1/p} \tag{15.49}$$

To identify the function Φ present in (15.36), we observe from (15.41) that $\varphi(\Phi(f)) = f$. Therefore if we in (15.49) adopt $x = \Phi(f)$ we obtain

$$\sigma_{yo}\left(\frac{\Phi(f)}{\eta D}\right)^{1/p} = f$$

which leads to

$$\boxed{\Phi(f) = \eta D\left(\frac{f}{\sigma_{yo}}\right)^{p}} \tag{15.50}$$

Therefore, if the function $\Phi(f)$ is chosen in this fashion the Cowper-Symonds model (15.48) is retrieved.

Led by expression (15.50), we choose

$$\boxed{\Phi(f) = \eta D\left(\frac{f}{\sigma_{yo} + K(\varepsilon_{eff}^{vp})}\right)^{p}} \tag{15.51}$$

Insertion into (15.46) gives

$$f = [\sigma_{yo} + K(\varepsilon_{eff}^{vp})](\frac{\dot{\varepsilon}_{eff}^{vp}}{D})^{1/p}$$

and use of (15.44) results in

$$\sigma_{eff} = \sigma_{st}(\varepsilon_{eff}^{vp})[1 + (\frac{\dot{\varepsilon}_{eff}^{vp}}{D})^{1/p}] \tag{15.52}$$

where the static stress-strain curve is given by $\sigma_{st}(\varepsilon_{eff}^{vp}) = \sigma_{yo} + K(\varepsilon_{eff}^{vp})$. Also expression (15.52) is often used to fit experimental data.

Here, we have discussed the implications of the choices (15.50) and (15.51) and we refer to Perzyna (1966) for further interpretations and possibilities.

The rather detailed discussion above was based on the simple model provided by isotropic hardening von Mises formulation (15.44) and it is evident that a number of other possibilities exists; in fact, to each of the plasticity models discussed in Chapters 12 and 13 there exists a corresponding viscoplastic model. We will not pursue this line any further, but simply mention that the Armstrong-Frederick model discussed in detail in Section 13.3 forms the basis of a number of very successful models used to simulate the complex creep behavior in the gas-turbine and nuclear industry. As an example, we refer to the formulations proposed by Chaboche (1989, 1993a) as well as Chaboche and Nouailhas (1989) and also dealt with in the textbook of Lemaitre and Chaboche (1990).

15.4.2 Duvaut-Lions viscoplasticity

Having discussed Perzyna-viscoplasticity in detail, we now turn to the other major approach which is provided by Duvaut and Lions (1972).

The driving force in viscoplasticity is the overstress, which is a measure of how far we are outside the static yield surface $f = 0$. In Perzyna viscoplasticity, this measure is provided by determination of the scalar $f(\sigma_{ij}, K_\alpha)$, i.e. evaluating the static yield function at the current state.

Referring to the uniaxial case shown in Fig. 15.21a), we could equally well measure the overstress as the stress difference between the current stress and the stress at the static stress-strain curve. In the general situation shown in Fig. 15.21b), the overstress is taken as the stress difference $\sigma_{ij} - \bar{\sigma}_{ij}$ where $\bar{\sigma}_{ij}$ is a stress value at the static yield surface $f = 0$. This leads to the *Duvaut-Lions formulation* given by

$$\dot{\varepsilon}_{ij}^{vp} = \frac{1}{\eta}(\sigma_{ij} - \bar{\sigma}_{ij}) \tag{15.53}$$

where η is a constant viscosity parameter. The original Duvaut-Lions model applies to ideal viscoplasticity where no hardening parameters exist and (15.53)

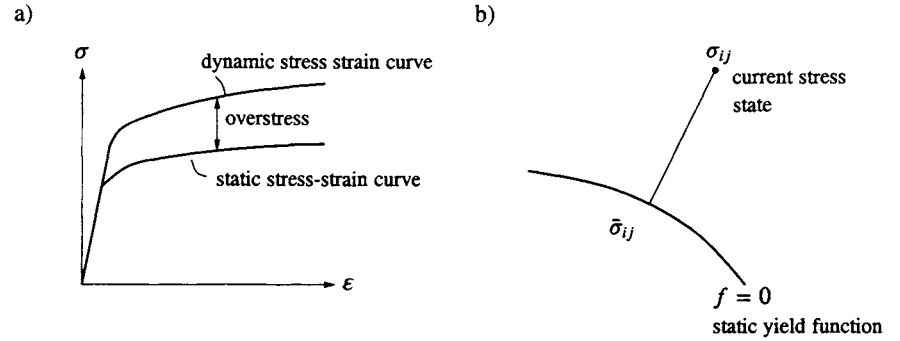

Figure 15.21: Illustration of Duvaut-Lions viscoplasticity based on overstress; a) uniaxial situation, b) overstress $\sigma_{ij} - \bar{\sigma}_{ij}$ in the general situation.

is the only evolution law. It remains to define the stress state $\bar{\sigma}_{ij}$ located on the static yield surface which for ideal viscoplasticity takes the format $f(\bar{\sigma}_{ij}, \bar{K}_\alpha = 0) = F(\bar{\sigma}_{ij}) = 0$. In the Duvaut-Lions model, the $\bar{\sigma}_{ij}$-value is taken as the *closest-point-projection* of the current stress state on the static yield surface $F(\bar{\sigma}_{ij}) = 0$. Let us discuss the concept of the closest-point-projection in more detail.

Considering a point in a space, this point can be projected on a surface such that the distance between the point and its projection on the surface is as small as possible; this constitutes the closest-point-projection. Now, any space possesses a *metric* which controls how distances are measured. In Euclidean space, the metric tensor is given by Kronecker's delta δ_{ij} such that the quadratic form $s^2 = x_i \delta_{ij} x_j$ measures the squared distance between the start and end point of the vector x_i. In the original Duvaut-Lions formulation, the $\bar{\sigma}_{ij}$-value is determined as the Euclidean closest-point-projection on the static yield surface $F(\bar{\sigma}_{ij}) = 0$.

When the Duvaut-Lions formulation is generalized to include hardening viscoplasticity, the static yield surface now also depends on the hardening parameters and it seems reasonable to measure the distance between the current state and the static yield surface not only expressed in terms of stresses, but also in terms of hardening parameters; following Simo *et al.* (1988) we will now see how this generalization can be achieved.

The static yield function is given by $f(\sigma_{ij}, K_\alpha)$. Similar to (15.37), the hardening parameters K_α are related to the internal variables κ_α through $K_\alpha = K_\alpha(\kappa_\beta)$ which leads to

$$\boxed{\dot{K}_\alpha = d_{\alpha\beta}\dot{\kappa}_\beta \quad \textit{where} \quad d_{\alpha\beta} = \frac{\partial K_\alpha}{\partial \kappa_\beta}} \tag{15.54}$$

Thermodynamic considerations discussed later in Chapter 22 show that the ma-

trix $d_{\alpha\beta}$ is symmetric. Its inverse matrix $c_{\alpha\beta}$ fulfills per definition the expression $c_{\alpha\gamma}d_{\gamma\beta} = \delta_{\alpha\beta}$ and (15.54) then leads to

$$\boxed{\dot{\kappa}_\alpha = c_{\alpha\beta}\dot{K}_\beta}$$

As usual, C_{ijkl} denotes the elastic flexibility tensor, cf. (4.26). It is now assumed that the metric tensor in the σ_{ij}, K_α - space is defined by

$$\begin{bmatrix} C_{ijkl} & 0 \\ 0 & c_{\alpha\beta} \end{bmatrix} \tag{15.55}$$

In the σ_{ij}, K_α - space, the distance s between the state σ_{ij}, K_α and the state $\bar{\sigma}_{ij}, \bar{K}_\alpha$ is, per definition, given by

$$s^2 = \frac{1}{2}(\sigma_{ij} - \bar{\sigma}_{ij})C_{ijkl}(\sigma_{kl} - \bar{\sigma}_{kl}) + \frac{1}{2}(K_\alpha - \bar{K}_\alpha)c_{\alpha\beta}(K_\beta - \bar{K}_\beta) \tag{15.56}$$

where the factor $1/2$ has been introduced for convenience; a more detailed discussion is given by Ristinmaa and Ottosen (1998).

In the discussion leading to (10.14) it was mentioned that, for plasticity, the second law of thermodynamics is expressed as $\sigma_{ij}\dot{\varepsilon}^p_{ij} - K_\alpha\dot{\kappa}_\alpha \geq 0$. It then follows that the quantities $\sigma_{ij}C_{ijkl}\sigma_{kl}$ and $K_\alpha c_{\alpha\beta}K_\beta$ are of the same dimension [Nm/m^3] and this supports the choice of the metric given by (15.55).

Let σ_{ij}, K_α be the current state and let $\bar{\sigma}_{ij}, \bar{K}_\alpha$ be some state of the static yield surface given by $f(\bar{\sigma}_{ij}, \bar{K}_\alpha) = 0$. Assuming both C_{ijkl} and $c_{\alpha\beta}$ to be constant quantities, we now determine the state $\bar{\sigma}_{ij}, \bar{K}_\alpha$ such that it becomes the closest-point-projection on the static yield surface. Therefore, for given σ_{ij}, K_α we want to determine the state $\bar{\sigma}_{ij}, \bar{K}_\alpha$ which minimizes the distance s^2 defined by (15.56) under the constraint at $f(\bar{\sigma}_{ij}, \bar{K}_\alpha) = 0$. The Lagrangian multiplier method is summarized in Appendix and (A.15) then provides

$$\begin{aligned} -C_{ijkl}(\sigma_{kl} - \bar{\sigma}_{kl}) + \mu\frac{\partial f}{\partial \bar{\sigma}_{ij}} &= 0 \\ -c_{\alpha\beta}(K_\beta - \bar{K}_\beta) + \mu\frac{\partial f}{\partial \bar{K}_\alpha} &= 0 \\ f(\bar{\sigma}_{ij}, \bar{K}_\alpha) &= 0 \end{aligned} \tag{15.57}$$

where μ is a non-negative Lagrangian multiplier. This equation system determines the unknowns $\bar{\sigma}_{ij}, \bar{K}_\alpha$ and μ.

With these preliminaries, we are now in a position to express generalized

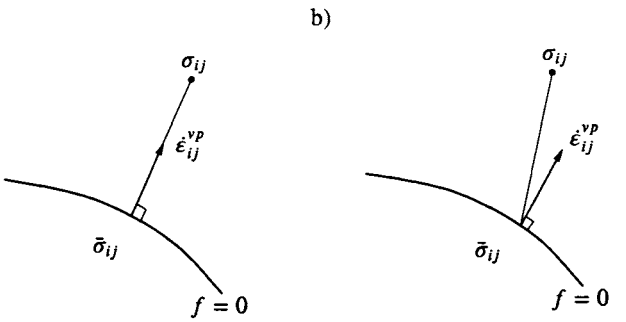

Figure 15.22: Ideal viscoplasticity. a) Duvaut-Lions formulation in stress space; b) Generalized Duvaut-Lions formulation in stress space.

Duvaut-Lions viscoplasticity according to

Generalized Duvaut-Lions viscoplasticity

$$\sigma_{ij} = D_{ijkl}(\varepsilon_{kl} - \varepsilon_{kl}^{vp})$$

if $f(\sigma_{ij}, K_\alpha) \leq 0$ *then*

$$\dot{\varepsilon}_{ij}^{vp} = 0 \quad \dot{\kappa}_\alpha = 0$$

if $f(\sigma_{ij}, K_\alpha) \geq 0$ *then*

$$\dot{\varepsilon}_{ij}^{vp} = \Lambda C_{ijkl}(\sigma_{kl} - \bar{\sigma}_{kl})$$

$$\dot{\kappa}_\alpha = -\Lambda c_{\alpha\beta}(K_\alpha - \bar{K}_\alpha)$$

where $f = f(\sigma_{ij}, K_\alpha)$ *is the static yield function and* $\bar{\sigma}_{ij}, \bar{K}_\alpha$ *is the closest-point-projection on the static yield surface* $f(\bar{\sigma}_{ij}, \bar{K}_\alpha) = 0$ (15.58)

Moreover, Λ is any positive quantity that we choose and it seems natural to let Λ depend on the distance s defined in (15.56). We shall see later that the formulation (15.58) is very attractive from a computational point of view.

To further explore the differences between the original Duvaut-Lions model and the generalized Duvaut-Lions formulation, the consequences of (15.53) are illustrated in Fig. 15.22a) showing the closest-point-projection in Euclidean space as well as the direction of $\dot{\varepsilon}_{ij}^{vp}$. In Fig. 15.22b), the generalized Duvaut-Lions formulation is shown where the closest-point-projection $\bar{\sigma}_{ij}$ is determined by the metric given in (15.55). As a comparison of (15.58) and (15.57) shows, it is of interest that $\dot{\varepsilon}_{ij}^{vp}$ is still orthogonal to the static yield surface $f = 0$.

Despite the differences in formulation, it turns out that there are cases where Perzyna and generalized Duvaut-Lions viscoplasticity coincide and a detailed investigation is provided by Runesson *et al.* (1999). As an illustration, take

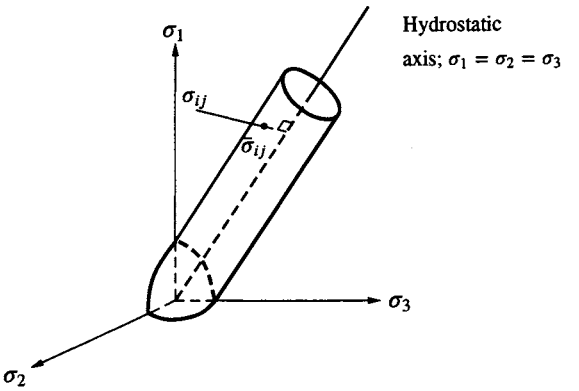

Figure 15.23: Closest point projection $\bar{\sigma}_{ij}$ of the current stress point σ_{ij} on the static yield surface in terms of a von Mises cylinder, the space is Euclidean.

the static yield function as an isotropic hardening von Mises formulation, i.e. $f = \sigma_{eff} - \sigma_{yo} - K$. Then (15.45) shows that Perzyna viscoplasticity is given by

$$\dot{\varepsilon}_{ij}^{vp} = \frac{\Phi(f)}{\eta} \frac{3s_{ij}}{2\sigma_{eff}} \tag{15.59}$$

Let the current stress state σ_{ij} be projected on the von Mises cylinder to obtain the Euclidean closest-point-projection $\bar{\sigma}_{ij}$ on the static yield surface as shown in Fig. 15.23. Since both σ_{ij} and $\bar{\sigma}_{ij}$ are located in the same deviatoric plane, we have $\sigma_{ij} - \bar{\sigma}_{ij} = s_{ij} - \bar{s}_{ij}$. Assuming isotropic elasticity, the flexibility tensor C_{ijkl} is given by (4.93) and we then obtain $C_{ijkl}(\sigma_{kl} - \bar{\sigma}_{kl}) = C_{ijkl}(s_{kl} - \bar{s}_{kl}) = (s_{ij} - \bar{s}_{ij})/2G$. Finally, we have $\bar{s}_{ij} = k s_{ij}$ where k is a proportionality factor which leads to $(s_{ij} - \bar{s}_{ij})/2G = (1 - k)s_{ij}/2G$, i.e. $C_{ijkl}(\sigma_{kl} - \bar{\sigma}_{kl}) = (1 - k)s_{ij}/2G$ and a comparison of (15.59) and (15.58) shows that by proper choice of, say, the Λ-quantity, the Perzyna and Duvaut-Lions formulations coincide.